

Current observations favour phantom-enhanced nature of dark energy

Md. Wali Hossain^{1,*}

¹*Department of Physics, Jamia Millia Islamia, New Delhi, 110025, India*

Our study shows that the more a dark energy model allows the equation of state to become phantom-like toward the past, the better it fits current observations which also may lead to stronger statistical tension with Λ CDM. In particular, models with greater flexibility in their redshift evolution, such as power-law type forms, are mildly preferred over more restrictive parametrizations with similar parameter dimensionality. For the dataset including DESY5, the deviation from Λ CDM reaches a significance of 6.26σ . These results indicate that present data are sensitive to enhanced phantom behaviour and provide clear guidance for constructing phenomenologically viable dark energy parametrizations.

I. INTRODUCTION

The standard Λ cold dark matter (Λ CDM) model, in which dark energy is described by a cosmological constant Λ , has been highly successful in explaining a wide range of cosmological observations, including the cosmic microwave background (CMB) [1]. However, increasingly precise data have revealed persistent tensions that challenge its internal consistency. Most notably, the Hubble constant inferred from Planck CMB measurements is in $\sim 5\sigma$ tension with local determinations by the SH0ES collaboration [1, 2]. Additionally, weak-lensing and large-scale structure measurements favour lower values of the clustering amplitude $S_8 = \sigma_8 \sqrt{\Omega_{m0}/0.3}$ than predicted by the CMB [3, 4]. More recently, baryon acoustic oscillation (BAO) data from DESI, when combined with Type Ia supernova (SNeIa) and CMB observations, have been shown to favour dynamical dark energy (DDE) over Λ CDM at the 2.6σ – 3.1σ level within the Chevallier–Polarski–Linder (CPL) framework [5–7]. These findings motivate a systematic exploration of dark energy parametrizations beyond Λ CDM.

In this context, DDE models, in which the equation of state (EoS) $w(a)$ evolves with cosmic time, provide a natural framework for addressing these observational tensions. Among the simplest and most widely studied examples is the CPL parametrization [8, 9], $w(a) = w_0 + w_a(1 - a)$, which offers a convenient and flexible description of dark energy dynamics at low redshifts, particularly for $z < 1$. Nevertheless, the CPL form may be inadequate to capture the true dynamics of dark energy, since it asymptotically approaches a constant value $w(a) \rightarrow w_0 + w_a$ at $z \gtrsim 1$, thereby motivating the exploration of alternative parametrizations [10–16].

Recently, Ref. [15] proposed a class of three-parameter dark energy EoS parametrizations. Despite the presence of an additional free parameter relative to CPL, these models achieve smaller minimum χ^2 values for data combinations including all three SNeIa samples. Dynamically, they exhibit a more pronounced phantom phase than CPL for certain values of (w_0, w_a) , a behaviour

that is also evident in the EoS evolution evaluated at the best-fit parameters. These findings point to an emerging trend among smooth dark energy parametrizations, such as CPL and those introduced in Ref. [15], where models with enhanced phantom behaviour are increasingly favoured by current observations. If this trend is robust, it may have several important implications:

1. dark energy may be more phantom-like than previously inferred;
2. the CPL parametrization may become inadequate near $z \sim 1$ or at higher redshifts;
3. this behaviour may guide the construction of parametrizations that better capture the true dynamics of dark energy, reducing arbitrariness in phenomenological modeling;
4. such models may exhibit increased statistical tension with the Λ CDM scenario.

In this work, we investigate these possibilities in detail. In addition to the CPL model, we consider two well studied two-parameter parametrizations, the Barboza–Alcaniz (BA) model [10] and the exponential (EXP) model [11]. To further extend our analysis, we introduce two additional two-parameter forms, the power-law (PL) parametrization, $w(a) = w_0/a^\alpha$, and its generalization, the modified power-law (MPL) parametrization, $w(a) = w_0/(1+a^\alpha)$. These monotonic parametrizations introduce no additional free parameters beyond those of CPL, while allowing for a more flexible evolution of the dark energy EoS, particularly beyond the low-redshift regime where the CPL expansion is expected to be valid.

II. MODELS

As discussed in the introduction, we consider the well-studied CPL, BA, and EXP parametrizations, whose dark energy equations of state are given by

$$w(a) = w_0 + w_a(1 - a), \quad (\text{CPL}), \quad (1)$$

$$w(a) = w_0 + w_a \frac{1 - a}{a^2 + (1 - a)^2}, \quad (\text{BA}), \quad (2)$$

* mhossain@jmi.ac.in

$$w(a) = w_0 + w_a(e^{1-a} - 1), \quad (\text{EXP}), \quad (3)$$

where a is the scale factor.

The CPL parametrization provides flexibility only at low redshifts ($z \ll 1$). To allow greater freedom at higher redshifts, we introduce a simple extension of the w CDM model in which, instead of being a constant, the EoS evolves as a power law,

$$w(a) = w_0 a^{-\alpha} = w_0(1+z)^\alpha, \quad (4)$$

where α is a free parameter. For $\alpha > 1$, this form diverges as $a \rightarrow 0$, but this does not affect our analysis since current observations probe only the low-redshift regime. To regularize the high-redshift behaviour while retaining the enhanced flexibility at low and intermediate redshifts, we further introduce a modified power-law (MPL) form,

$$w(a) = \frac{2w_0}{1+a^\alpha}, \quad (5)$$

which asymptotically approaches $w(a) \rightarrow 2w_0$ as $a \rightarrow 0$. While this fixed asymptotic value introduces a dynamical restriction, it is again irrelevant for present data. Both parametrizations can be further generalized by introducing an additional parameter,

$$w(a) = \frac{(1+\beta)w_0}{\beta+a^\alpha}, \quad (6)$$

where β controls the asymptotic behaviour of the equation of state at high redshift. In this work, we restrict our analysis to the two representative cases $\beta = 0$ and $\beta = 1$, corresponding to the PL and MPL forms, respectively.

For $z \ll 1$, both PL and MPL reduce to the CPL form with $w(a=1) = w_0$ and

$$w_{a,\text{PL}} = - \left. \frac{dw}{da} \right|_{a=1} = \alpha w_0, \quad (7)$$

$$w_{a,\text{MPL}} = - \left. \frac{dw}{da} \right|_{a=1} = \frac{\alpha w_0}{2}. \quad (8)$$

The corresponding dark energy density evolution for the PL model is

$$\rho_{\text{DE,PL}}(z) = \rho_{\text{DE},0}(1+z)^3 \exp\left[\frac{3w_0}{\alpha}((1+z)^\alpha - 1)\right], \quad (9)$$

which reduces to the w CDM form in the limit $\alpha \rightarrow 0$. For the MPL model, the dark energy density evolves as

$$\rho_{\text{DE,MPL}}(z) = \rho_{\text{DE},0}(1+z)^3 \left(\frac{1+(1+z)^\alpha}{2}\right)^{\frac{6w_0}{\alpha}}, \quad (10)$$

recovering the w CDM scaling as $\alpha \rightarrow 0$ and yielding $\rho_{\text{DE}} \propto (1+z)^{3+6w_0}$ at very high redshifts, consistent with the asymptotic limit $w \rightarrow 2w_0$.

Figure 1 compares the evolution of $\rho(z)$ and $w(z)$ for the PL, MPL, and CPL parametrizations using identical values of w_0 and w_a . While all models agree at very

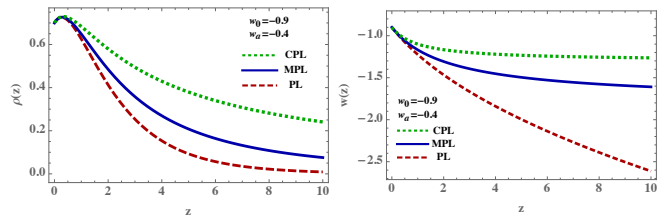


FIG. 1. Left: Dark energy density $\rho(z)$ is plotted against redshift z for PL, MPL and CPL. Right: The corresponding EoS ($w(z)$) is plotted against z . Both panels use identical values of w_0 and w_a for all models.

low redshifts, the PL and MPL parametrizations rapidly deviate from CPL at higher redshifts, exhibiting a significantly enhanced phantom behaviour. This illustrates the restrictive nature of retaining only the first-order Taylor expansion in CPL and highlights the increased dynamical freedom of the power-law based models.

III. DATA ANALYSIS

We constrain several dark energy models using the latest cosmological observations, including Λ CDM, CPL, PL, MPL, as well as the BA and EXP parametrizations.

For the Λ CDM model, we vary six cosmological parameters, $\{\Omega_{\text{m}0}, h, \omega_{\text{b}}, r_{\text{d}}h, \sigma_8, M\}$, where $\omega_{\text{b}} = \Omega_{\text{b}0}h^2$ is the physical baryon density, r_{d} is the comoving sound horizon at the baryon drag epoch, and M denotes the absolute magnitude of SNeIa. Uniform priors are imposed as $\Omega_{\text{m}0} \in [0.2, 0.5]$, $h \in [0.5, 0.8]$, $\omega_{\text{b}} \in [0.005, 0.05]$, $r_{\text{d}}h \in [60, 140]$, $\sigma_8 \in [0.5, 1.0]$, and $M \in [-22, -15]$. The same priors on the common cosmological parameters are adopted for all extended dark energy models.

The PL and MPL parametrizations introduce two additional dark energy parameters, α and w_0 . For the PL model, we adopt uniform priors $\alpha \in [-1, 2]$ and $w_0 \in [-2, 1]$ for all data combinations. For the MPL model, we use $\alpha \in [-1, 6]$ and $w_0 \in [-2, 1]$.

The CPL, BA, and EXP models share the same dark energy parametrization in terms of w_0 and w_a . For these models, we impose uniform priors $w_0 \in [-2, 0]$ and $w_a \in [-2, 1]$ for all data sets.

We perform a Markov Chain Monte Carlo (MCMC) analysis to constrain the model parameters using the publicly available EMCEE sampler [17]. The resulting chains are analysed and visualised with the GetDist package [18]. Convergence of the MCMC chains is assessed using the Gelman–Rubin statistic [19], requiring $|R - 1| \lesssim 0.01$.

A. Observational Data

Our analysis combines multiple cosmological probes, including CMB, BAO, SNeIa, Hubble parameter mea-

measurements, and redshift-space distortion (RSD) data.

For the CMB, we use distance priors reconstructed from the Planck 2018 TT, TE, EE+lowE measurements [1, 20], together with the Planck determination of the physical baryon density, ω_b [1].

The BAO dataset is taken from DESI DR2 [6], comprising over 14 million extragalactic objects, including emission line galaxies (ELGs), luminous red galaxies (LRGs), quasars (QSOs) [21], and Ly α forest tracers [22]. These measurements provide D_M/r_d and D_H/r_d over $0.4 < z < 4.2$, along with low-redshift isotropic measurements of D_V/r_d for $0.1 < z < 0.4$, thereby covering both isotropic and anisotropic BAO analyses.

For type Ia supernovae, we use the PantheonPlus compilation, containing 1550 luminosity distance measurements spanning $0.001 < z < 2.26$ [23, 24]. We also include the Union3 compilation [25], which provides 22 binned data points from 2087 cosmologically useful SNeIa, and the DESY5 sample [26], consisting of 1635 SNeIa in the range $0.10 < z < 1.13$, supplemented by 194 low-redshift SNeIa ($0.025 < z < 0.10$), for a total of 1829 data points.

We further include 31 measurements of the Hubble parameter $H(z)$ spanning $0.07 \leq z \leq 1.965$, obtained using the cosmic chronometer (CC) method [27]. Finally, we incorporate RSD measurements of the growth rate $f\sigma_8(z)$ compiled in [28], constructing the covariance matrix and χ^2 statistic accordingly.

We consider three data combinations corresponding to different SNeIa samples. The combination CMB+DESI DR2+H(z)+RSD+PantheonPlus is denoted as +PantheonPlus. Similarly, CMB+DESI DR2+H(z)+RSD+Union3 is referred to as +Union3, and CMB+DESI DR2+H(z)+RSD+DESY5 as +DESY5.

B. Model selection and statistical tension

To assess and compare the performance of different dark energy models, we employ standard model selection criteria [29–31], namely the Akaike Information Criterion (AIC) [32] and the Bayesian Information Criterion (BIC) [33]. These are defined as $\text{AIC} = \chi_{\min}^2 + 2N$ and $\text{BIC} = \chi_{\min}^2 + N \ln k$, where χ_{\min}^2 is the minimum chi-squared value, N denotes the number of free parameters, and k is the total number of data points. The relative performance of a model with respect to Λ CDM is quantified through $\Delta\text{AIC} = \text{AIC}_{\text{model}} - \text{AIC}_{\Lambda\text{CDM}}$ and $\Delta\text{BIC} = \text{BIC}_{\text{model}} - \text{BIC}_{\Lambda\text{CDM}}$, with negative (positive) values indicating preference for (disfavouring of) the model relative to Λ CDM.

The statistical tension between two models, A and B , is quantified using the Mahalanobis distance squared statistic [34] together with Wilks' theorem [35], following [15] by the p -value, $p = 1 - F_{\chi^2}(\Delta\chi^2; k)$, where $\Delta\chi^2 = (\boldsymbol{\mu}_A - \boldsymbol{\mu}_B)^T \mathbf{C}^{-1} (\boldsymbol{\mu}_A - \boldsymbol{\mu}_B)$ follows a χ^2 distribution with k degrees of freedom, where $\boldsymbol{\mu}_i$ and \mathbf{C}_i are

the mean vectors and covariance matrices obtained from the MCMC posteriors, and the combined covariance is $\mathbf{C} = \mathbf{C}_A + \mathbf{C}_B$. p is expressed as an equivalent Gaussian significance, $\sigma_{\text{eq}} = \Phi^{-1}(1 - p/2)$, where Φ^{-1} denotes the inverse cumulative distribution function (CDF) of the standard normal distribution. In one dimension ($k = 1$), the tension is given by $\sigma_{\text{eq}} = |\mu_{A,j} - \mu_{B,j}| / \sqrt{\sigma_{A,j}^2 + \sigma_{B,j}^2}$. For a two-dimensional subspace ($k = 2$), the corresponding 2×2 covariance sub-matrices are used, with $\Delta\chi^2(\theta_1, \theta_2) = (\boldsymbol{\mu}_A - \boldsymbol{\mu}_B)^T (\mathbf{C}_A^{2 \times 2} + \mathbf{C}_B^{2 \times 2})^{-1} (\boldsymbol{\mu}_A - \boldsymbol{\mu}_B)$, and the associated p -values and σ_{eq} are computed from a χ^2 distribution with $k = 2$ degrees of freedom.

IV. RESULTS

Upper panel of Table I summarises the cosmological parameter constraints for Λ CDM and the DDE models considered in this work, namely PL, MPL, CPL, BA, and EXP, using the +PantheonPlus, +Union3, and +DESY5 data combinations. Across all datasets, the background parameters Ω_{m0} , H_0 , ω_b , $r_d h$, σ_8 , and the absolute magnitude M are broadly consistent among the models, with only minor variations (Fig. 2). The +DESY5 combination yields slightly higher values of H_0 and lower Ω_{m0} compared to the +PantheonPlus and +Union3 samples. As illustrated in Fig. 2, the introduction of DDE primarily affects the dark energy sector, leaving the background parameters largely unchanged. The lower panel of Table I summarises the cosmological tension between Λ CDM model and the DDE models.

For the dark energy EoS, as shown in Table I and the Figs. 3 and 4, all DDE models exhibit clear deviations from the Λ CDM value $w = -1$, with a well-defined hierarchy emerging in the evolution of DDE. Although the CPL and MPL models generally favour more negative best-fit values of w_a than the PL model, their evolution is intrinsically restricted by the requirement that $w(z)$ approaches a fixed asymptotic value already at low or intermediate redshifts as shown in Fig. 1. This restriction limits the depth of the phantom phase, causing the evolution to effectively saturate beyond a narrow redshift range (Fig. 4). The BA model behaves similarly, as its functional form also enforces convergence to a fixed asymptotic value, suppressing the further departure from $w = -1$ as depicted in Fig. 4. In contrast, the PL parametrization is free from such asymptotic constraints. Even with comparatively less negative values of w_a , this freedom allows $w(z)$ to evolve more rapidly away from CPL-like behaviour, producing a deeper and more extended phantom phase (Figs. 1 and Fig. 4). The EXP model occupies an intermediate position, while it is constrained to reach a fixed EoS only at very high redshifts, it retains substantial freedom at low and intermediate redshifts, leading to a phantom evolution that is stronger than in CPL, MPL, and BA, but weaker than in PL as shown in the Fig. 4.

TABLE I. Cosmological parameter constraints (68% CL) and tension analysis for Λ CDM and DDE models (PL, MPL, CPL, BA, and EXP) using the +PantheonPlus, +Union3, and +DESY5 data combinations.

Model/Dataset	Ω_{m0}	H_0	$\omega_b \times 10^3$	rah	σ_8	M	DE Parameters					
ΛCDM												
+PantheonPlus	0.3087 ± 0.0059	67.89 ± 0.45	22.45 ± 0.13	100.39 ± 0.51	0.75 ± 0.029	-19.425 ± 0.013	$w = -1$ (fixed)					
+Union3	0.3072 ± 0.0060	68.00 ± 0.47	22.48 ± 0.13	100.50 ± 0.53	0.751 ± 0.029	...	$w = -1$ (fixed)					
+DESY5	0.2784 ± 0.0021	70.46 ± 0.16	22.98 ± 0.10	102.98 ± 0.27	0.783 ± 0.030	...	$w = -1$ (fixed)					
PL												
+PantheonPlus	0.3123 ± 0.0066	67.71 ± 0.61	22.40 ± 0.15	99.71 ± 0.86	0.751 ± 0.029	-19.415 ± 0.016	$\alpha = 0.382 \pm 0.153$ $w_0 = -0.880 \pm 0.048$ $w_a = -0.330 \pm 0.120$ $\alpha = 0.642 \pm 0.205$					
+Union3	0.3211 ± 0.0083	66.80 ± 0.78	22.41 ± 0.15	98.20 ± 1.16	0.7486 ± 0.0291	...	$w_0 = -0.778 \pm 0.067$ $w_a = -0.487 \pm 0.123$ $\alpha = 0.747 \pm 0.145$					
+DESY5	0.2984 ± 0.0040	68.98 ± 0.38	22.60 ± 0.136	100.77 ± 0.65	0.77 ± 0.03	...	$w_0 = -0.788 \pm 0.042$ $w_a = -0.584 \pm 0.089$					
MPL												
+PantheonPlus	0.3128 ± 0.0067	0.6766 ± 0.0062	0.022405 ± 0.000147	99.67 ± 0.87	0.7511 ± 0.0292	-19.4164 ± 0.0160	$\alpha = 0.998 \pm 0.494$ $w_0 = -0.868 \pm 0.054$ $w_a = -0.422 \pm 0.186$ $\alpha = 2.876 \pm 1.402$					
+Union3	0.3231 ± 0.0079	0.6656 ± 0.0077	0.022419 ± 0.000148	97.98 ± 1.09	0.7481 ± 0.0286	...	$w_0 = -0.710 \pm 0.082$ $w_a = -0.969 \pm 0.384$ $\alpha = 2.922 \pm 1.104$					
+DESY5	0.2980 ± 0.0034	0.6895 ± 0.0036	0.022626 ± 0.000132	100.85 ± 0.60	0.7704 ± 0.0298	...	$w_0 = -0.738 \pm 0.059$ $w_a = -1.048 \pm 0.320$					
CPL												
+PantheonPlus	0.3126 ± 0.0067	67.60 ± 0.63	22.41 ± 0.15	99.69 ± 0.89	0.752 ± 0.029	-19.418 ± 0.016	$w_0 = -0.862 \pm 0.059$ $w_a = -0.53^{+0.24}_{-0.21}$					
+Union3	0.3224 ± 0.0087	66.6 ± 0.82	22.42 ± 0.15	98.1 ± 1.2	0.748 ± 0.021	...	$w_0 = -0.717 \pm 0.089$ $w_a = -0.97 \pm 0.30$					
+DESY5	0.2989 ± 0.0043	68.85 ± 0.41	22.61 ± 0.14	100.74 ± 0.68	0.77 ± 0.021	...	$w_0 = -0.721 \pm 0.057$ $w_a = -1.17^{+0.24}_{-0.22}$					
BA												
+PantheonPlus	0.3125 ± 0.0067	67.67 ± 0.63	22.42 ± 0.15	99.74 ± 0.87	0.750 ± 0.029	-19.417 ± 0.016	$w_0 = -0.884 \pm 0.050$ $w_a = -0.260 \pm 0.107$					
+Union3	0.3224 ± 0.0088	66.66 ± 0.82	22.42 ± 0.15	98.11 ± 1.20	0.747 ± 0.029	...	$w_0 = -0.762 \pm 0.077$ $w_a = -0.456 \pm 0.146$					
+DESY5	0.2984 ± 0.0043	68.97 ± 0.40	22.61 ± 0.14	100.87 ± 0.67	0.769 ± 0.029	...	$w_0 = -0.779 \pm 0.049$ $w_a = -0.541 \pm 0.112$					
EXP												
+PantheonPlus	0.3125 ± 0.0066	67.67 ± 0.61	22.41 ± 0.15	99.70 ± 0.85	0.750 ± 0.029	-19.416 ± 0.016	$w_0 = -0.873 \pm 0.053$ $w_a = -0.408 \pm 0.170$					
+Union3	0.3224 ± 0.0089	66.66 ± 0.83	22.40 ± 0.15	98.07 ± 1.22	0.748 ± 0.029	...	$w_0 = -0.743 \pm 0.083$ $w_a = -0.720 \pm 0.232$					
+DESY5	0.2992 ± 0.0042	68.90 ± 0.40	22.60 ± 0.13	100.72 ± 0.67	0.770 ± 0.029	...	$w_0 = -0.753 \pm 0.052$ $w_a = -0.861 \pm 0.172$					
Tension Analysis												
Dataset	PL		MPL			CPL		BA		EXP		
	(w_0)	(w_0, w_a)	(α, w_0)	(w_0)	(w_0, w_a)	(α, w_0)	(w_0)	(w_0, w_a)	(w_0)	(w_0, w_a)	(w_0)	(w_0, w_a)
+PantheonPlus	2.50σ	2.31σ	2.11σ	2.46σ	2.01σ	1.98σ	2.33σ	1.92σ	2.32σ	1.98σ	2.41σ	2.01σ
+Union3	3.28σ	3.55σ	2.85σ	3.51σ	3.41σ	4.16σ	3.16σ	2.76σ	3.09σ	2.74σ	3.10σ	2.72σ
+DESY5	5.14σ	6.26σ	4.98σ	4.23σ	4.34σ	5.55σ	4.83σ	4.70σ	4.51σ	4.51σ	4.79σ	4.71σ

This hierarchy is directly reflected in the statistical inference summarised in Table II. All DDE parametrizations improve the fit relative to Λ CDM, with substantial reductions in the minimum χ^2 , particularly for the +DESY5 dataset, where the PL model achieves $\Delta\chi^2 \simeq -39$ and the remaining models show comparable, though slightly weaker, improvements. The corresponding differ-

ences in AIC and BIC indicate a consistent preference for DDE. The tension analysis, reported in the lower panel of Table I, reinforces this picture, one-dimensional comparisons in w_0 yield tensions ranging from $\sim 2.3\sigma$ for PantheonPlus to $\sim 5\sigma$ for DESY5, while in the two-dimensional (w_0, w_a) space the tensions increase further, reaching up to 6.3σ for the PL model with DESY5. A no-

TABLE II. Statistical model comparison between Λ CDM and DDE models (PL, MPL, CPL, BA, and EXP).

Statistical Model Comparison															
Dataset	Λ CDM			PL				MPL				CPL			
	χ^2_{\min}	AIC	BIC	χ^2_{\min}	$\Delta\chi^2$	Δ AIC	Δ BIC	χ^2_{\min}	$\Delta\chi^2$	Δ AIC	Δ BIC	χ^2_{\min}	$\Delta\chi^2$	Δ AIC	Δ BIC
+PantheonPlus	1447.55	1459.55	1492.02	1440.49	-7.06	-3.06	7.76	1440.86	-6.69	-2.69	8.13	1441.33	-6.22	-2.22	8.60
+Union3	72.00	82.00	94.27	60.29	-11.71	-7.71	-2.80	60.95	-11.05	-7.05	-2.14	60.83	-11.17	-7.17	-2.26
+DES Y5	1731.10	1741.10	1768.83	1692.15	-38.94	-34.94	-23.85	1694.53	-36.58	-32.58	-21.48	1694.85	-36.25	-32.25	-21.16

Dataset	BA				EXP			
	χ^2_{\min}	$\Delta\chi^2$	Δ AIC	Δ BIC	χ^2_{\min}	$\Delta\chi^2$	Δ AIC	Δ BIC
+PantheonPlus	1441.07	-6.49	-2.49	8.33	1440.93	-6.62	-2.62	8.19
+Union3	60.86	-11.14	-7.14	-2.23	60.58	-11.42	-7.42	-2.51
+DES Y5	1694.62	-36.48	-32.48	-21.39	1693.28	-37.82	-33.82	-22.73

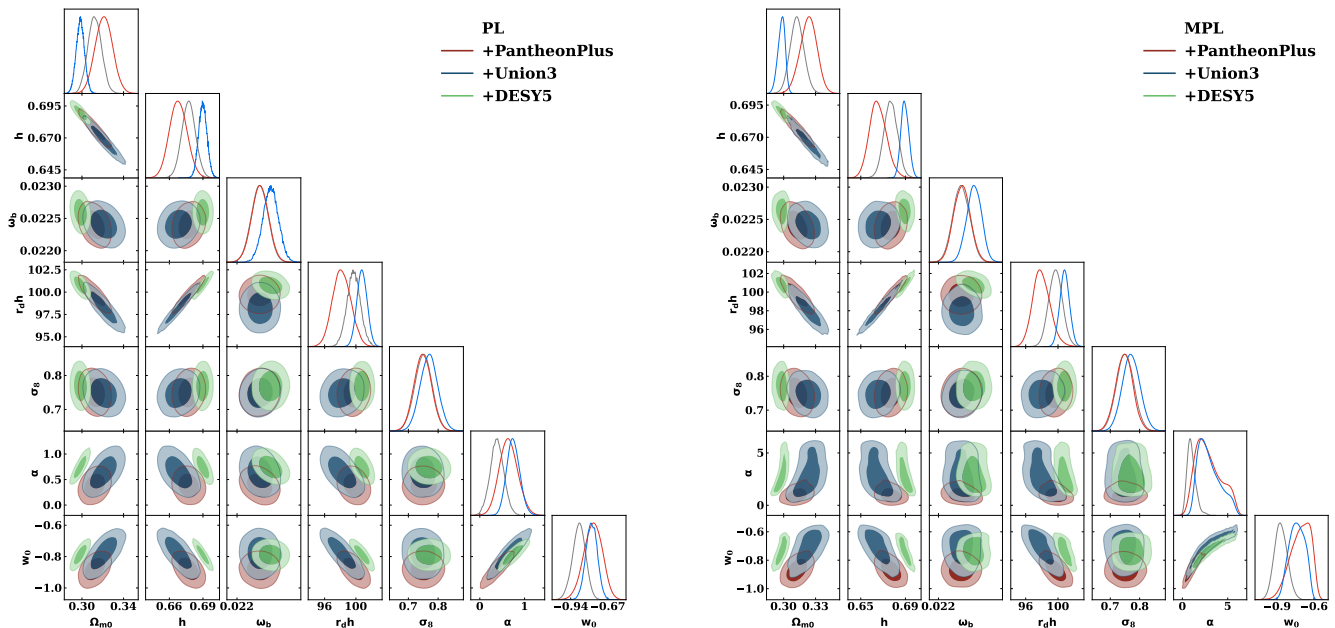
FIG. 2. 1σ and 2σ confidence contours for the parameters of PL (left) and MPL (right) models.

table feature of the PL and MPL parametrizations is that the tension associated with the (α, w_0) subspace is comparable to, and in some cases larger than, that obtained in (w_0, w_a) , indicating that α captures a genuinely global deviation from Λ CDM rather than a purely low-redshift effect. In contrast, w_a primarily encodes the local slope of the EoS near $z \simeq 0$, while α governs the overall redshift evolution of $w(z)$ across the observational range. Overall, parametrizations that allow a more extended and flexible phantom phase, most notably PL, and to a lesser extent EXP, lead simultaneously to improved goodness of fit and to larger statistical deviations from the Λ CDM scenario, whereas models with stronger asymptotic restrictions exhibit weaker tensions and reduced statistical preference.

V. CONCLUSIONS

Our analysis shows that current cosmological observations favour DDE models that allow a stronger departure into the phantom regime, rather than models that only cross the phantom divide. Although all the parametrizations considered remain phantom once $w(z) < -1$ is reached, the data prefer models in which the EoS evolves more strongly away from $w = -1$. This preference cannot be adequately captured by CPL-like expansions, whose validity is intrinsically limited to low redshifts. Instead, the data increasingly favour equations of state with greater dynamical freedom, achieved without introducing unnecessary complexity, thereby signalling a departure from standard CPL-type behaviour as one approaches and exceeds $z \sim 1$. To study this, we introduce two new

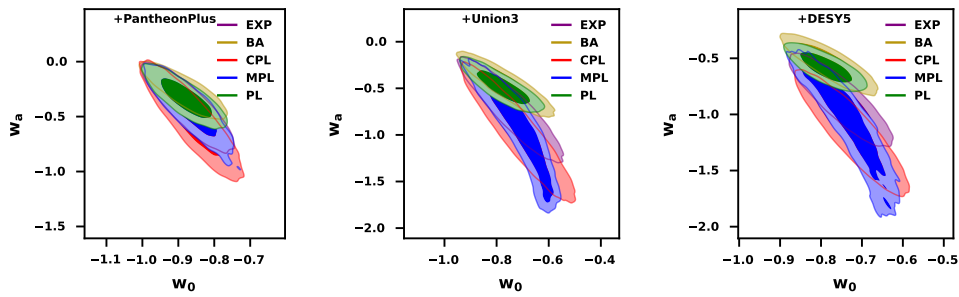


FIG. 3. 1σ and 2σ confidence contours for the parameters w_0 and w_a in the PL, MPL, CPL, BA and EXP models.

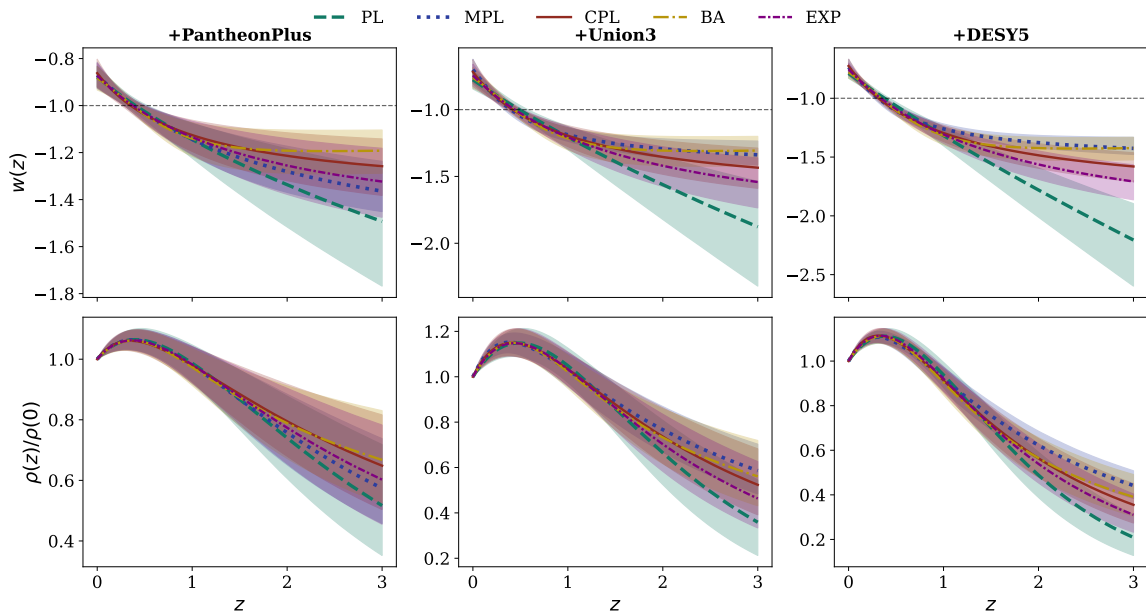


FIG. 4. Reconstructed EoS in PL, MPL, CPL, BA and EXP models with the median value (lines) and 1σ errors (shaded region).

parametrizations, the PL and MPL forms, which naturally allow for a stronger and more persistent phantom phase than commonly used two-parameter models.

We performed a comprehensive comparison of Λ CDM, PL, MPL, CPL, BA, and EXP models using the +PantheonPlus, +Union3, and +DESY5 data combinations. Among all DDE scenarios considered, the PL parametrization emerges as the most strongly favoured by the data (Table II). It consistently yields the largest reduction in χ^2 and the most competitive information criteria, while simultaneously driving the reconstructed EoS deeper into the phantom regime across cosmic time (Fig. 4). In contrast, the MPL parametrization behaves similarly to CPL and BA, as its enforced approach to a constant asymptotic value restricts the late-time dynamics and limits the extent of phantom evolution, thereby reducing its statistical preference. The EXP model occupies an intermediate position (Fig. 4). It also approaches

a constant EoS but this occurs only at very high redshifts, allowing for greater freedom at low and intermediate redshifts and leading to a more pronounced phantom phase than CPL, MPL, or BA, but still weaker than that achieved by PL.

Crucially, we find that enhanced phantom evolution is systematically accompanied by an increase in statistical tension with Λ CDM. For the +DESY5 data combinations, the inferred deviations reach and exceed the 5σ level, establishing a direct and robust connection between improved goodness of fit, extended phantom behaviour, and growing cosmological tension. This result indicates that present observations are sensitive not merely to departures from $w = -1$, but to the structure of the dark energy evolution itself, preferentially selecting models that amplify phantom behaviour over cosmic time.

Taken together, these findings suggest that the era of largely arbitrary dark energy parametrizations is drawing

to a close. Current data now impose clear phenomenological requirements that a viable models of cosmic acceleration must permit enhanced phantom evolution while maintaining controlled complexity. This provides a de-

cisive direction for future model building and represents a significant step toward uncovering the true nature of cosmic acceleration.

-
- [1] N. Aghanim *et al.* (Planck), *Astron. Astrophys.* **641**, A6 (2020), [Erratum: *Astron.Astrophys.* 652, C4 (2021)], [arXiv:1807.06209 \[astro-ph.CO\]](#).
- [2] A. G. Riess *et al.*, *Astrophys. J. Lett.* **934**, L7 (2022), [arXiv:2112.04510 \[astro-ph.CO\]](#).
- [3] L. Perivolaropoulos and F. Skara, *New Astron. Rev.* **95**, 101659 (2022), [arXiv:2105.05208 \[astro-ph.CO\]](#).
- [4] T. M. C. Abbott *et al.* (Kilo-Degree Survey, Dark Energy Survey), *Open J. Astrophys.* **6**, 2305.17173 (2023), [arXiv:2305.17173 \[astro-ph.CO\]](#).
- [5] A. G. Adame *et al.* (DESI), *JCAP* **02**, 021, [arXiv:2404.03002 \[astro-ph.CO\]](#).
- [6] M. Abdul Karim *et al.* (DESI) (2025), [arXiv:2503.14738 \[astro-ph.CO\]](#).
- [7] G. Gu *et al.* (DESI) (2025), [arXiv:2504.06118 \[astro-ph.CO\]](#).
- [8] M. Chevallier and D. Polarski, *Int. J. Mod. Phys. D* **10**, 213 (2001), [arXiv:gr-qc/0009008](#).
- [9] E. V. Linder, *Phys. Rev. Lett.* **90**, 091301 (2003), [arXiv:astro-ph/0208512](#).
- [10] E. M. Barboza, Jr. and J. S. Alcaniz, *Phys. Lett. B* **666**, 415 (2008), [arXiv:0805.1713 \[astro-ph\]](#).
- [11] N. Dimakis, A. Karagiorgos, A. Zampeli, A. Paliathanasis, T. Christodoulakis, and P. A. Terzis, *Phys. Rev. D* **93**, 123518 (2016), [arXiv:1604.05168 \[gr-qc\]](#).
- [12] L. Feng and T. Lu, *Journal of Cosmology and Astroparticle Physics* **2011** (11), 034–034.
- [13] J.-Z. Ma and X. Zhang, *Phys. Lett. B* **699**, 233 (2011), [arXiv:1102.2671 \[astro-ph.CO\]](#).
- [14] H. K. Jassal, J. S. Bagla, and T. Padmanabhan, *Mon. Not. Roy. Astron. Soc.* **356**, L11 (2005), [arXiv:astro-ph/0404378](#).
- [15] S. Alam and M. W. Hossain (2025), [arXiv:2510.03779 \[astro-ph.CO\]](#).
- [16] S. Akthar and M. W. Hossain, *JCAP* **04**, 024, [arXiv:2411.15892 \[astro-ph.CO\]](#).
- [17] D. Foreman-Mackey, D. W. Hogg, D. Lang, and J. Goodman, *Publ. Astron. Soc. Pac.* **125**, 306 (2013), [arXiv:1202.3665 \[astro-ph.IM\]](#).
- [18] A. Lewis (2019), [arXiv:1910.13970 \[astro-ph.IM\]](#).
- [19] A. Gelman and D. B. Rubin, *Statist. Sci.* **7**, 457 (1992).
- [20] L. Chen, Q.-G. Huang, and K. Wang, *JCAP* **2019**, 028 (2019), [arXiv:1808.05724 \[astro-ph.CO\]](#).
- [21] U. Andrade *et al.* (DESI) (2025), [arXiv:2503.14742 \[astro-ph.CO\]](#).
- [22] M. A. K. e. al., *Phys. Rev. D*, (2025), [arXiv:2503.14739 \[astro-ph.CO\]](#).
- [23] D. Scolnic *et al.*, *Astrophys. J.* **938**, 113 (2022), [arXiv:2112.03863 \[astro-ph.CO\]](#).
- [24] D. Brout *et al.*, *Astrophys. J.* **938**, 110 (2022), [arXiv:2202.04077 \[astro-ph.CO\]](#).
- [25] D. Rubin *et al.* (2023), [arXiv:2311.12098 \[astro-ph.CO\]](#).
- [26] T. M. C. Abbott *et al.* (DES), *Astrophys. J. Lett.* **973**, L14 (2024), [arXiv:2401.02929 \[astro-ph.CO\]](#).
- [27] A. Gómez-Valent and L. Amendola, *JCAP* **2018**, 051 (2018), [arXiv:1802.01505 \[astro-ph.CO\]](#).
- [28] S. Nesseris, G. Pantazis, and L. Perivolaropoulos, *Phys. Rev. D* **96**, 023542 (2017), [arXiv:1703.10538 \[astro-ph.CO\]](#).
- [29] A. R. Liddle, P. Mukherjee, and D. Parkinson (2006), [arXiv:astro-ph/0608184](#).
- [30] K. Shi, Y. Huang, and T. Lu, *Mon. Not. Roy. Astron. Soc.* **426**, 2452 (2012), [arXiv:1207.5875 \[astro-ph.CO\]](#).
- [31] R. Trotta (2017), [arXiv:1701.01467 \[astro-ph.CO\]](#).
- [32] H. Akaike, *IEEE Transactions on Automatic Control* **19**, 716 (1974).
- [33] G. Schwarz, *Annals Statist.* **6**, 461 (1978).
- [34] P. C. Mahalanobis, *Proc. Natl. Inst. Sci. India* **2**, 49 (1936).
- [35] S. S. Wilks, *The Annals of Mathematical Statistics* **9**, 60 (1938).